

## 2D interpretation of self-potential data using Normalized Full Gradient, a case study: galena deposit

M. ABEDI<sup>1</sup>, M.K. HAFIZI<sup>2</sup> AND G.H. NOROUZI<sup>1</sup>

<sup>1</sup>Faculty of Mining Engineering, University of Tehran, Iran

<sup>2</sup>Institute of Geophysics, University of Tehran, Iran

(Received: May 9, 2011; accepted: December 14, 2011)

**ABSTRACT** This paper describes usage of the Normalized Full Gradient (NFG) method to self-potential (SP) data. It can be used to estimate location, depth to the top, and center of the deposit. One of the important parameters to estimate, the accurate shape of the deposit, is true selection of the harmonic number. In this paper, the correct harmonic number is determined by the trial-and-error method, and then this method would be tested for noise-corrupted synthetic data. As a consequence of using the NFG method to anomalies of simple geometric-shaped models including vertical sheet and inclined sheet, the underground structures are found very close to their actual locations. In order to see the capability of the method to localize multi-object simultaneously, the NFG method could accurately indicate location of both constructed structures along a profile. Subsequently, reasonable results are acquired after corrupting the anomalies with noise. Finally, the NFG is applied to SP data from a galena deposit located in the NW of Iran, Khalf village. Geological interpretation of the study area confirmed occurrence of a Galena vein. The vein deposit can be simulated by a simple sheet model. After implementation of the method, a general view of the deposit structure is obtained and it helped us to get a fast interpretation. Final result of this method showed that the deposit began from the surface to approximately less than 50 m.

**Key words:** SP data, NFG method, synthetic models, Khalf's galena deposit.

### 1. Introduction

The self-potential (SP) data, as an old geophysical method that provides important information about near surface structures, has various applications in the mineral prospecting related to sulphide and graphite (Yungul, 1950; Tlas and Asfahani, 2007), groundwater investigation (Buselli and Kanglin, 2001) and determination of the subsurface temperature distributions (Friedel *et al.*, 2004).

Many numerical approaches such as least-squares method (Abdelrahman and Sharafeldin, 1997; Abdelrahman *et al.*, 1997; Shalivahan *et al.*, 1998; Asfahani and Tlas, 2002, 2005; Tlas and Asfahani, 2007), spectral analysis (Atchuta *et al.*, 1982; Sundararajan *et al.*, 1990, 1998; Akgün *et al.*, 1996; Sundararajan and Srinivas, 1996), derivative analysis (Abdelrahman *et al.*, 1998, 2003), curve matching techniques (Rao and Babu, 1983; Babu and Rao, 1988; El-Araby, 2004) and neural network (El-Kaliouby and Al-Garni, 2009) were applied to interpret SP anomalies.

In this study, the Normalized Full Gradient (NFG) method that was expressed firstly by Sindirgi *et al.* (2008) to interpret SP anomalies of simple sources is used. They applied the NFG to identify

three simple shape bodies such as sphere, horizontal cylinder and vertical sheet. The NFG is a powerful method in determination of the underground structures for gravity and magnetic prospecting that was firstly developed for these geophysical methods. The main reason to use the NFG is downward continuation maps. Analytical downward continuation is a method of estimating the field closer to the source, and consequently, it results in a better resolution of underground rock distribution. The NFG as one of the best approaches for locating reservoirs from gravity data was proposed by Berezkin (1967, 1973, 1998) designated as the NFG. Xiao (1981) and Xiao and Zhang (1984) used the NFG for oil exploration in China. The method had been used by the Chinese in different oil fields. In the early 1990s, new efforts to apply the method to the high-precision gravity data were initiated. Zeng *et al.* (2002) published the results of using the method for 2D sections of anticlines with homogenous density in the Shengli oil field (Ardestani, 2004).

Initially, the geophysical prospecting was performed using SP method to localize Galena occurrence in the East-Azerbaijan province of Iran. Since the geological structure of the Galena deposit in this study corresponds to vein, application of the NFG method has been extended to new simple geometric-shaped models involving vertical sheet, inclined sheet and hybrid models in order to simulate its shape.

Based on acquiring acceptable results of using the NFG method for synthetic sheet structures, real SP field data of galena deposit located in the Khalf village is interpreted along four profiles. Satisfactory results are obtained in comparison with previous studies. Depth range varies from 5 m to less than 60 m.

## 2. The NFG method

The 2D NFG of geophysical anomalies is defined as (Berezkin, 1973),

$$G_H(x, z) = \frac{G(x, z)}{G_{CP}(z)} = \frac{\sqrt{V_x^2(x, z) + V_z^2(x, z)}}{\frac{1}{S} \sum_0^S \sqrt{V_x^2(x, z) + V_z^2(x, z)}} \quad (1)$$

where  $G_H(x, z)$  is the NFG at point  $(x, z)$  on a cross-section  $x$ - $z$ ;  $V_z(x, z)$  and  $V_x(x, z)$  are the first vertical derivative and the first horizontal (along the  $x$ -direction) derivative of SP anomalies  $V$  at point  $(x, z)$ , respectively;  $G(x, z)$  is the full (total) gradient of SP anomalies at point  $(x, z)$ ;  $G_{CP}(z)$  is the average of the full gradient of SP anomalies at level  $z$  ( $z$  is a constant and CP is the abbreviation for average in Russian); and  $S$  is the number of samples in a data set. Eq. (1) shows that normalization means the full gradient  $G(x, z)$  is divided by the average  $G_{CP}(z)$  and the NFG is dimensionless (Zeng *et al.*, 2002).

The calculation of the NFG operator is accomplished by utilizing a Fourier series approach in which the  $V(x, z)$  function along the  $x$  axis between  $(-L, L)$  interval was given as (Bracewell, 1984; Blakely, 1995; Sindirgi *et al.*, 2008) follows:

$$V(x, z) = \sum_{n=0}^{\infty} [A_n \cos(\pi n / L)x + B_n \sin(\pi n / L)x] e^{(\pi n z / L)} \quad (2)$$

where the exponential term  $e^{(\pi n z/L)}$  corresponds to the change in  $V(x, z)$  along the  $z$  axis,  $A_n, B_n$  are Fourier coefficients and  $n$  is the harmonic or wave number. If the data are definitive in the  $(0, L)$  interval, then only the cosine or sine expansion can be used (Berezkin, 1973; Rikitake *et al.*, 1976; Sindirgi *et al.*, 2008). If the data have zero values at both end points in this interval, a faster approach can be obtained to the Fourier sine series. Therefore, a linear trend ( $a+bx$ ) is subtracted from the data values in the  $(0, L)$  interval. Here  $a$  is the beginning value of the  $V(x)$  function and  $b=(V(L)-V(0))/L$ . So, Berezkin (1973) expressed this anomalies over the range  $(-L, L)$  by the finite Fourier sine series

$$V(x, z) = \sum_{n=1}^K [B_n \sin(\pi n / L) x] e^{(\pi n z/L)} \quad (3)$$

where

$$B_n = \frac{2}{L} \int_0^L V(x, 0) \sin\left(\frac{\pi n}{L} x\right) dx \quad (4)$$

where  $K$  is the number of terms of the series. From Eq. (3), it follows that

$$V_x(x, z) = \frac{\pi}{L} \sum_{n=1}^K [n B_n \cos(\pi n / L) x] e^{(\pi n z/L)} \quad (5)$$

$$V_z(x, z) = \frac{\pi}{L} \sum_{n=1}^K [n B_n \sin(\pi n / L) x] e^{(\pi n z/L)}. \quad (6)$$

Defining a smoothing factor for eliminating high-frequency noise resulting from downward continuation, we finally have

$$q = \left[ \sin\left(\frac{\pi n}{N}\right) / \frac{\pi n}{N} \right]^m \quad (7)$$

where  $m$  is known as the degree of smoothing. The behaviour of the  $q$  equation as a function of harmonic number and damping parameter,  $m$ , is indicated in Fig. 1.

It was suggested choosing  $m$  equal to 1 or 2 to reach reasonable results (Aydin, 1997, 2010; Karsli, 2001; Dondurur, 2005). It is assumed equal to 1 in this study. Finally,

$$V(x, z) = \sum_{n=1}^K [B_n \sin(\pi n / L) x] e^{(\pi n z/L)} \left[ \sin\left(\frac{\pi n}{N}\right) / \frac{\pi n}{N} \right]^m \quad (8)$$

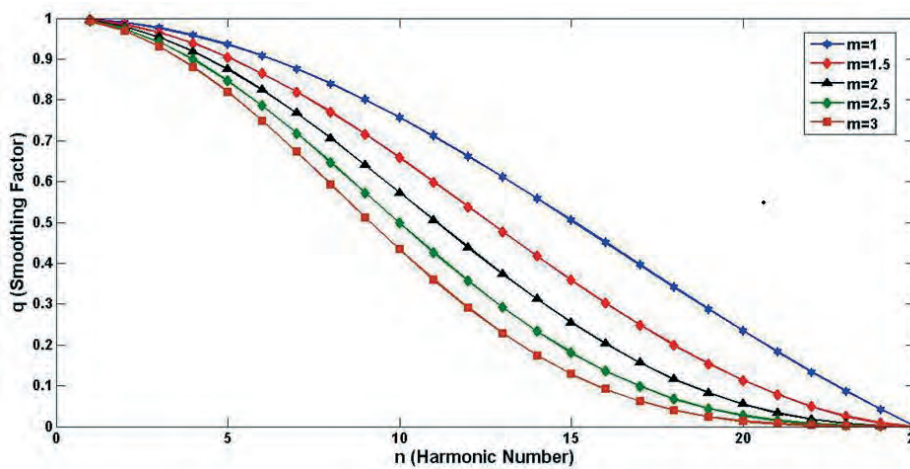


Fig. 1 - Behaviour of q function.

$$V_x(x, z) = \frac{\pi}{L} \sum_{n=1}^K [n B_n \cos(\pi n / L) x] e^{(\pi n z / L)} \left[ \sin\left(\frac{\pi n}{N}\right) / \frac{\pi n}{N} \right]^m \tag{9}$$

$$V_z(x, z) = \frac{\pi}{L} \sum_{n=1}^K [n B_n \sin(\pi n / L) x] e^{(\pi n z / L)} \left[ \sin\left(\frac{\pi n}{N}\right) / \frac{\pi n}{N} \right]^m \tag{10}$$

Substituting Eqs. (9) and (10) into Eq. (1), the NFG is calculated. The main issue to implement the NFG method is determining the harmonic number. It was selected by trial-and-error procedure in the most recent published papers (Ardestani, 2004).

The method is especially useful for detecting characteristic points of underground bodies such as centres and corners from singular points in the SP field.

### 3. Application to synthetic models

This section presents application of the NFG method to theoretical data from simple geometric-shaped models namely sheet. The profile length is chosen as 100 m, whereby the model location corresponded to the midpoint of profiles. Formulations of these structures are as follows.

#### 3.1. Vertical sheet

SP anomaly of this model was defined by (Rao and Babu, 1983) as

$$V(x) = k \log_e \left( \frac{x^2 + h^2}{(x^2 + H^2)} \right), k = \frac{\rho I}{2\pi} \tag{11}$$

where  $h$  and  $H$  are the upper and lower depth for edges of the model,  $k$  is the polarization parameter,

$\rho$  is the resistivity of the medium and  $I$  is the current density (current per unit area) of the medium. Assumed parameters in Table 1 are used to produce SP anomaly corrupted by 5% random noise (Fig. 2a). The number of optimal harmonic is determined by the trial-and-error method. There is no appropriate method to choose optimal harmonic numbers. Therefore, after applying several harmonics, the NFG map that identifies the most compact body from closed contours can be belonged to optimal harmonics.

Four harmonic numbers are used to map the NFG with assuming  $m$  equal to 1 (Figs. 2b to 2e). It is observed that closed contours around the body are produced for harmonics 10, 15 and 20. Best model usually has compact contours, and high values of the NFG correspond to anomaly source. The main point of using the NFG is that lower and higher harmonics could show deeper and shallower structures respectively (Sindirgi *et al.*, 2008; Aydin, 2010). Depth ranges of a synthetic vertical sheet can be determined approximately by the NFG cross-sections from various harmonic numbers. Indeed, cross-sections of the NFG map in Figs. 2b to 2e indicate approximate depth ranges of synthetic model. Furthermore, it is an issue to determine exact edges of sources by the NFG. It needs to interpret several cross-sections of the NFG simultaneously to overcome it. Therefore, approximate depths of the vertical sheet can be determined by consideration of various closed contours caused by the method. Fig. 2c shows upper and lower depth of the vertical sheet reasonably but upper depth (near to Earth surface) is indicated by increasing of the harmonics to 15 and 20. It is confirmed that lower harmonic numbers could localize deeper sources rather than higher ones (Sindirgi *et al.*, 2008; Aydin, 2010).

It is a negative point of the NFG method that one cannot justify quantitatively which of the harmonics is optimal. The best harmonic can be easily obtained at several numbers by the trial-and-error method. The results will be accepted when closed contours are produced in cross-sections. The geological background of the study area can help the interpreters as well. If a wrong harmonic is chosen, the high values of contours are not closed. Therefore, depth ranges cannot be interpreted causing misleading interpretation. For instance, it is shown in Fig. 2b.

### 3.2. Inclined sheet

The SP anomaly generated by an inclined sheet, that is shown in Fig. 3, is given by Rao and Babu (1983) as

$$V(x) = k \log_e \left( \frac{x^2 + h^2}{((x-a)^2 + H^2)} \right), \quad k = \frac{\rho I}{2\pi} \quad (12)$$

Assumed parameters are shown in Table 1. The noise level equal to 5% is added to produce SP anomaly. Four harmonic numbers involving 5, 10, 15, and 20 are used, while best model similar to

Table 1 - Assumed parameters for synthetic models.

Model	k (mV)	h (m)	H (m)	$\theta^\circ$	a (m)	Noise (%)
Vertical Sheet	100	2	12			5
Inclined Sheet	100	2	10	60	4.62	5

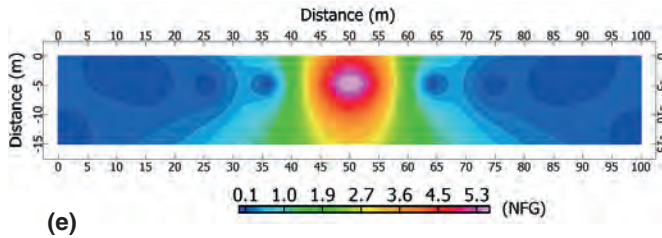
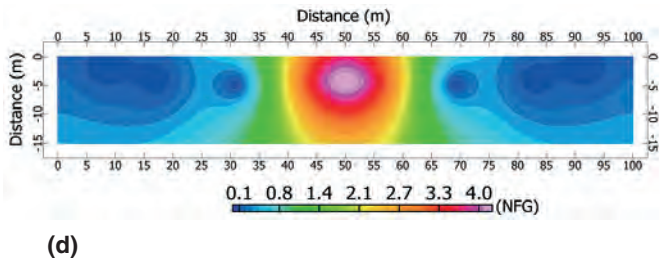
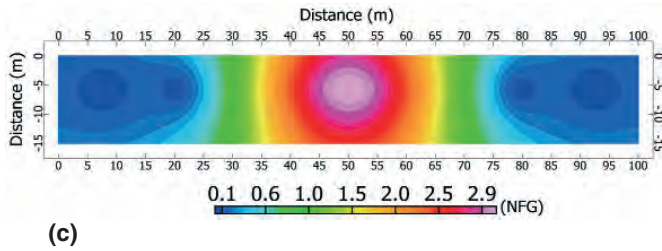
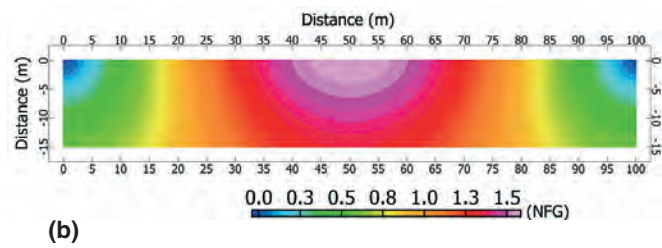
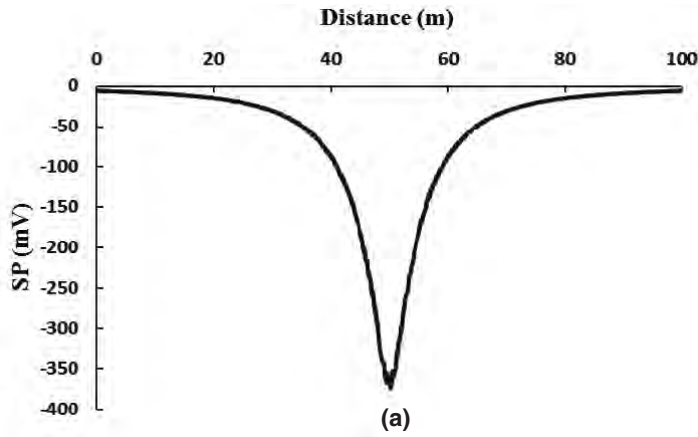


Fig. 2 - SP modeling for vertical sheet structure, a) SP anomaly along  $x$  axis, b) NFG map for  $n=5$ , c) NFG map for  $n=10$ , d) NFG map for  $n=15$ , e) NFG map for  $n=20$ .

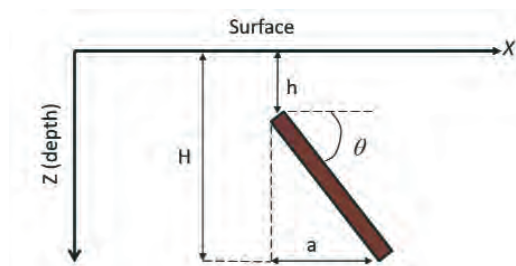


Fig. 3 - Cross-section of 2D thin inclined sheet model.

real model is obtained for harmonic numbers 10. Depth range can be identified approximately 2 to 10 m (Fig. 4c). Higher harmonics of 15 and 20 solely determine upper depth of synthetic inclined sheet. As is said, there is an inverse relation between number of harmonics and depth of sources.

All mentioned models were assumed to be single at midpoint of  $x$  profile, but in reality multi-object can produce SP anomaly. Therefore, multi-source SP anomaly is examined in the hybrid model.

### 3.3. Hybrid model

In order to examine the performance of the NFG for multi-object, two additional theoretical models are evaluated. Assumed parameters belonged to different locations of both models (vertical and inclined sheets) are shown in Table 2. The parameter  $x_0$  shows the location of sheets along  $x$  axis. Cross-sections of the NFG at different harmonic numbers are shown in Fig. 5. The level of added noise is 3% for both bodies. It is clear from Figs. 5b to 5e that both sheets locations correspond to their real locations at all harmonic numbers. The point is that the depth ranges of vertical sheet correspond to the reality but lower depth of inclined sheet is not identified by use of the NFG. Both models are delineated remarkably at harmonic number 10 in Fig. 5b whereas their upper depths are determined at higher harmonics of 15, 20, and 25.

## 4. Geology of the study area

The study area is located in the East-Azerbaijan province of Iran (Fig. 6). There is a galena prospect near Khalf village. It is 5 km far from the village. In Fig. 7, the geological map of the study area has been shown with 1:250,000 in scale. The survey area belongs to the geological period of Paleogene, and hydrothermal magmatic activities in the region are more recognizable. There is no faulting in this area according to the geological map and observations. The only fault that can be seen

Table 2 - Assumed parameters for synthetic hybrid model.

Multi-object		h (m)	H (m)	k (mV)	$x_0$ (M)	$\theta^\circ$	a (m)	Noise (%)
Model 1	Vertical Sheet	1	10	100	30			3
Model 2	Inclined Sheet	2	14	100	70	80	2.12	3

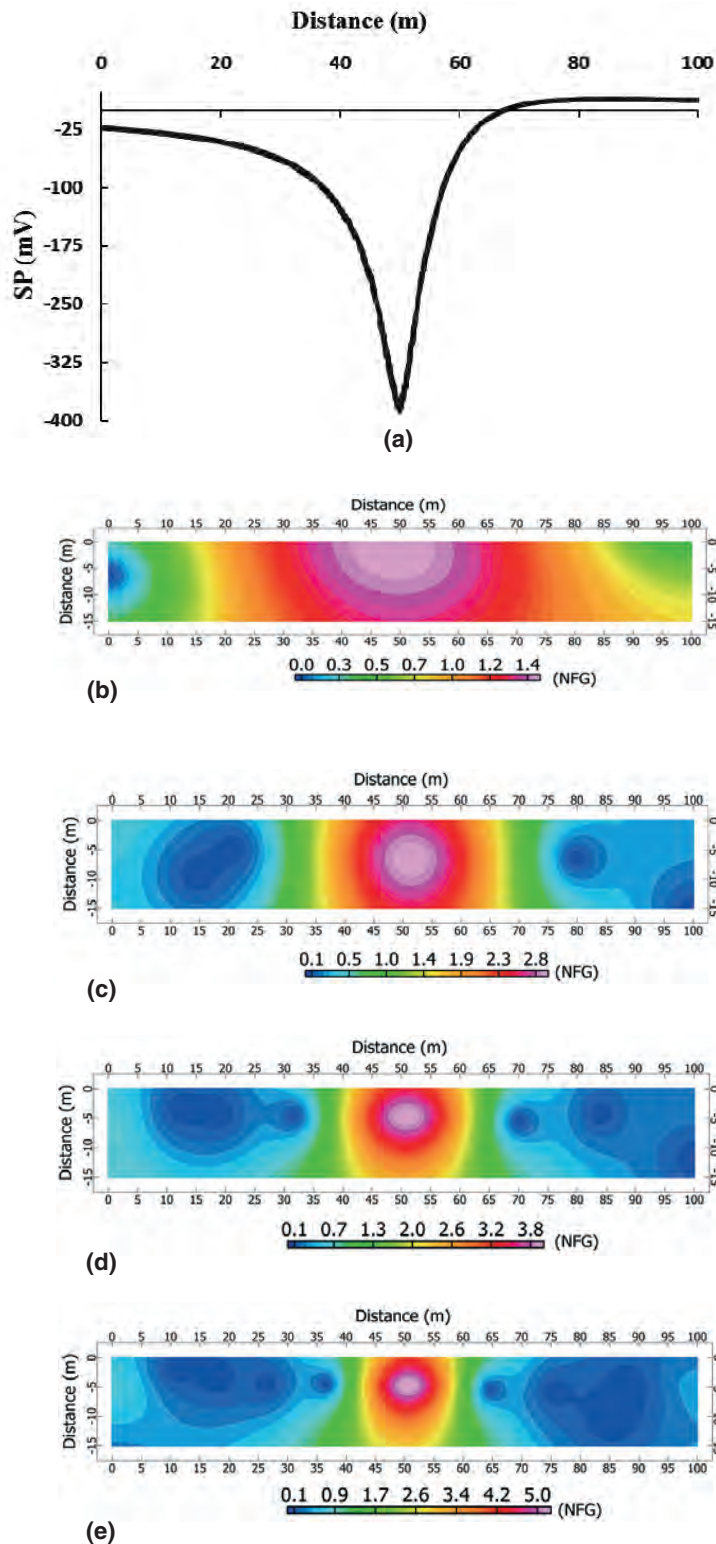


Fig. 4 - SP modeling for inclined sheet structure, a) SP anomaly along x axis, b) NFG map for  $n=5$ , c) NFG map for  $n=10$ , d) NFG map for  $n=15$ , e) NFG map for  $n=20$ .



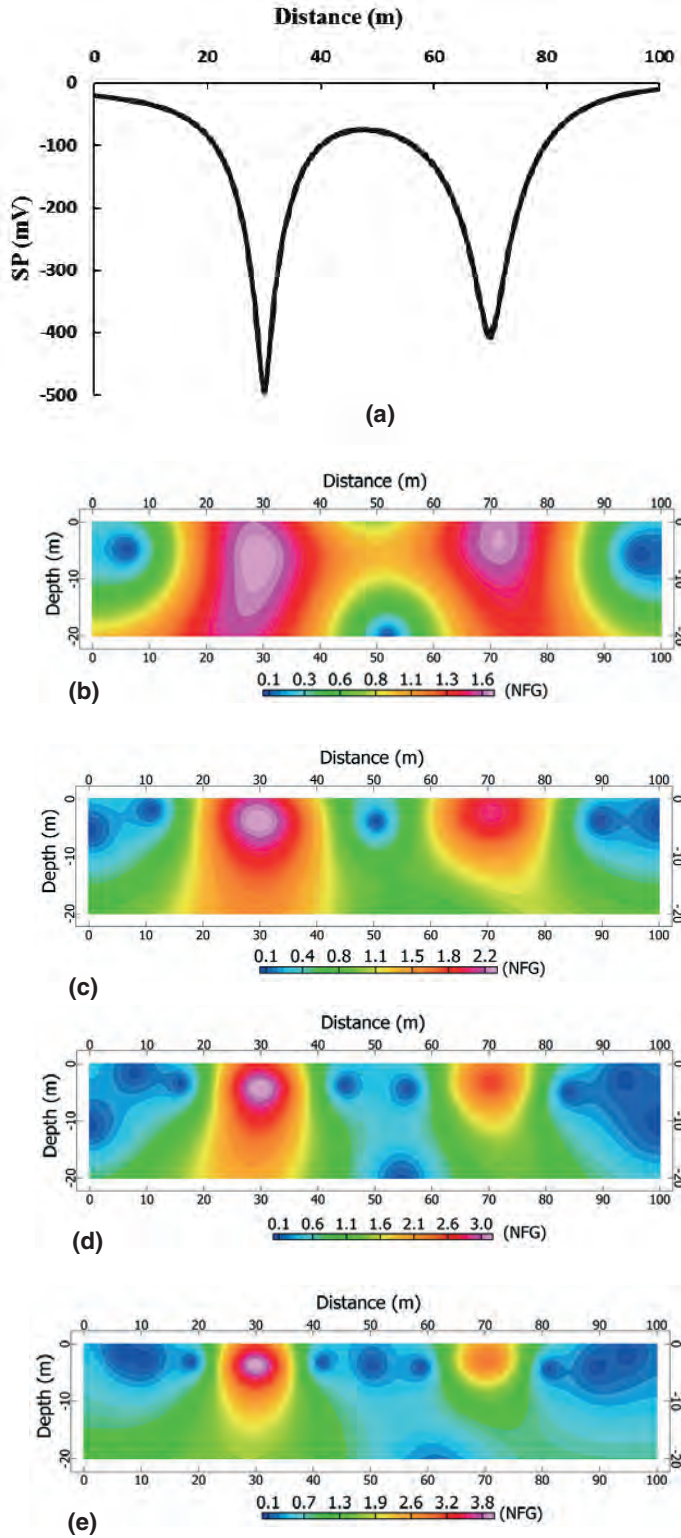


Fig. 5 - SP modeling for multi-object, a) SP anomaly along  $x$  axis, b) NFG map for  $n=10$ , c) NFG map for  $n=15$ , d) NFG map for  $n=20$ , e) NFG map for  $n=25$ .



Fig. 6 - Geographic location of study area in the map of Iran.

on the map is near Tazeh kand village, 5 km far from it. It is located among Karaj, Ziarat, and Fajan formations especially in Karaj and all of them belong to Paleogene. Thickness of Ziarat formation which is dominated by limestone is up to 1200 m. The Karaj formation is much thicker and its volcanic lavas are mainly andesite. In general, the main lithological units exposed in the area comprise of andesitic tuffs, tuffaceous sediments, andesitic lavas, rare red beds and acid tuffs, and thin nummulitic limestones. Its main mineral occurrences are related to Pb, Zn and Cu ore bodies, which generally are associated with volcanic and igneous activities in Paleogene. Some unimportant traces of mineral occurrences such as iron, coal, gypsum were observed as well (Esmaaili Oqaz, 1997).

## 5. Application of the NFG method to galena deposit

Eleven W-E-direction profiles with 25 m spacing are performed to cover the SP survey. Length of profiles is 310 m, whereby station spacing along each profile is 10 m. The SP measurement was done by the geoelectrical branch of the Institute of Geophysics, Tehran University, in 1996.

The SP anomaly caused by the galena deposit is mapped in Fig. 8. Geological interpretation indicates that galena ore body is exposed on the Earth surface in N-S direction, so the survey profiles

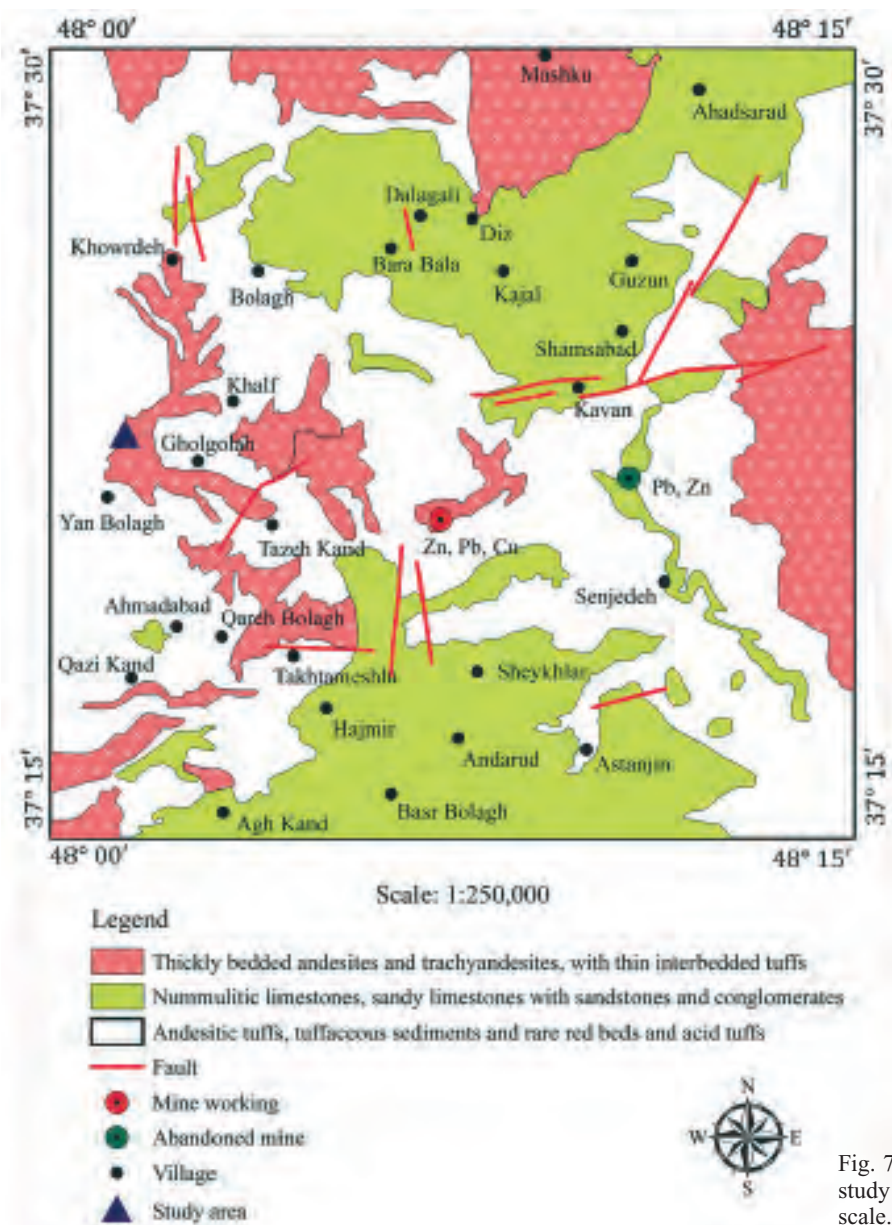


Fig. 7 - Geological map of the study area with 1: 250,000 in scale.

conducted W-E perpendicular to galena vein strike. Vein occurrence of galena can be simulated by sheet model, and as was confirmed, the NFG method properly detected synthetic sheet sources. Therefore, the 2D NFG method is applied to four profiles which are shown on the SP anomaly map in Fig. 8. The vein location corresponds to the distance about 140 m from origin of the W-E profiles in SP map. In addition to negative SP anomaly along the vein outcrop in Fig. 8, another remarkable SP anomaly that can belong to mineral occurrence exists in the north-eastern part of the study area.

Since there is no optimal approach to choose harmonic numbers, the NFG cross sections are mapped at four harmonic numbers including 10, 15, 20, and 25 chosen by the trial-and-error method.

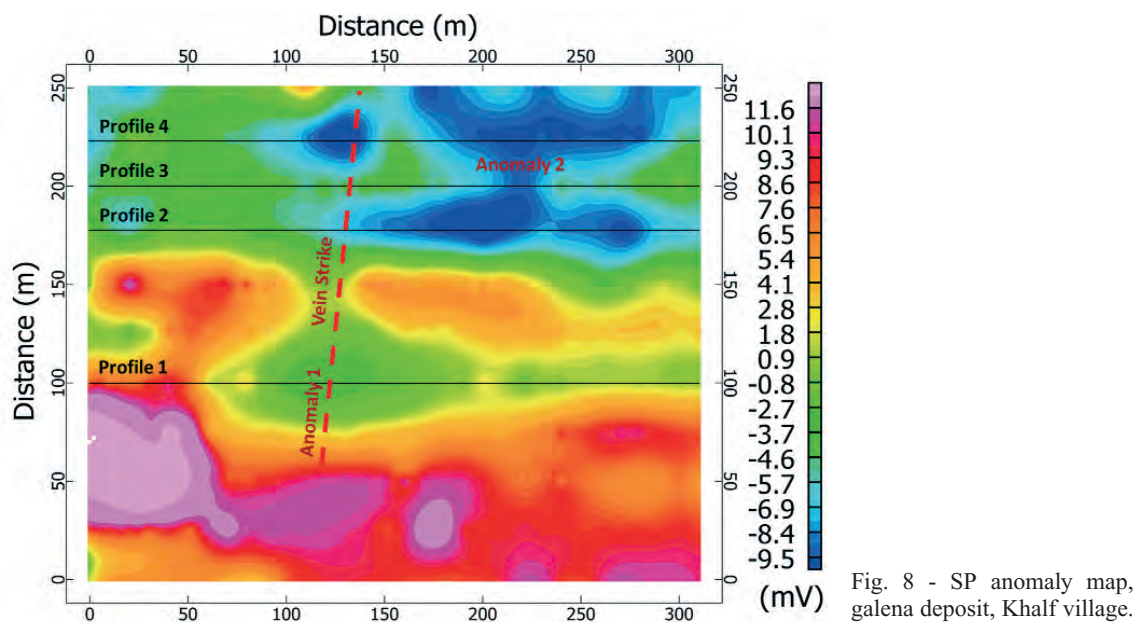


Fig. 8 - SP anomaly map, galena deposit, Khalf village.

The NFG cross-sections for depth ranges of 0 up to 100 m are shown in Figs 9 to 12. As it is known, SP data are really sensitive to noise, indeed their modeling results just can be used as a fast interpretation approach to acquire approximate information in concern with actual model parameters of mineral occurrence. Therefore, depth ranges are not exactly equal to real source depths.

By considering the NFG cross-sections at various harmonics in Fig. 9, high values of the NFG can be correlated with source location. SP anomaly along the profile 1 in Fig. 9a has negative values at its midpoint but the NFG cross-sections indicated the source location significantly shifted to the left side. Closed contours of the NFG map approximately show the center of source body. Therefore, based on the number of harmonics which can identify deeper and shallower sources, depth of galena vein can be from surface to less than approximately 50 m. Two major SP anomalies along profile 2, i.e., at distance 200 and 275 m from the beginning of the profile, are identified by the NFG cross sections in Figs. 10b to 10e. The NFG closed contours which indicate galena sources at distance 200 m are weaker than another one. Both of the galena probable sources have depth ranges from about 5 m to less than 50 m.

Two obvious negative anomalies along the profile 3 can be identified (Fig. 11a). The center locations of two underground structures from origin are approximately 100 and 225 m, respectively. Depth ranges of two bodies could be interpreted from NFG map based on the number of harmonics. The upper depth of both bodies can be identified 5 m and less than 5 m, respectively. Generally, the lower depth can be less than 50 m by considering the NFG map generated by various harmonic numbers. Finally, main negative SP anomaly along profile 4 indicates that source location corresponds to distance about 130 m from the origin, and depth ranges are from about 5 m to less than 50 m. Its NFG cross-sections are shown in Fig. 12b to 12e.

These results in comparison with other studies have reasonably matching. The main anomaly along profile 3 was modeled by an inclined sheet, in which depth varies from 5 m to less than 60 m

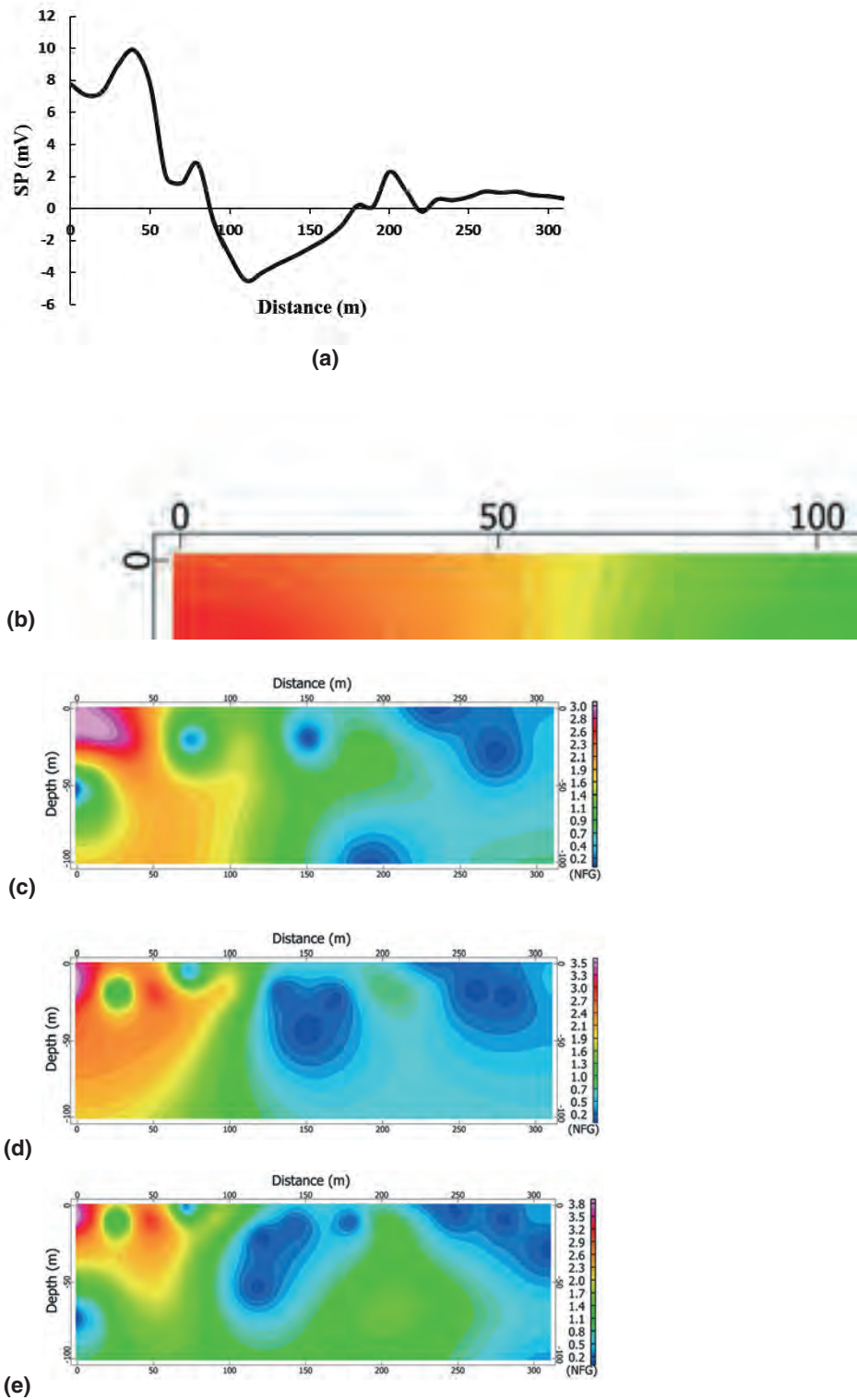


Fig. 9 - SP data modeling for profile 1, a) SP anomaly along  $x$  axis, b) NFG map for  $n=10$ , c) NFG map for  $m=15$ , d) NFG map for  $n=20$ , e) NFG map for  $n=25$ .

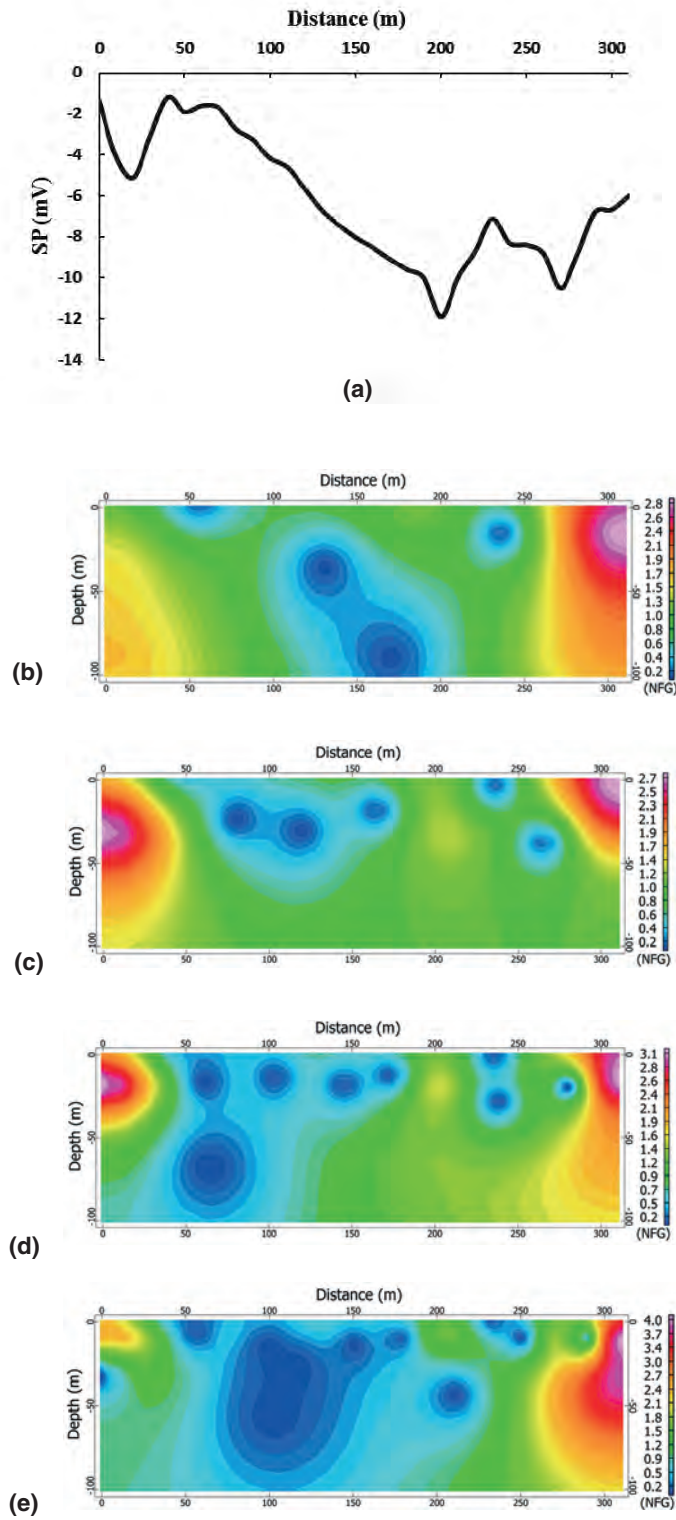


Fig. 10 - SP data modeling for profile 2, a) SP anomaly along  $x$  axis, b) NFG map for  $n=10$ , c) NFG map for  $n=15$ , d) NFG map for  $n=20$ , e) NFG map for  $n=25$ .

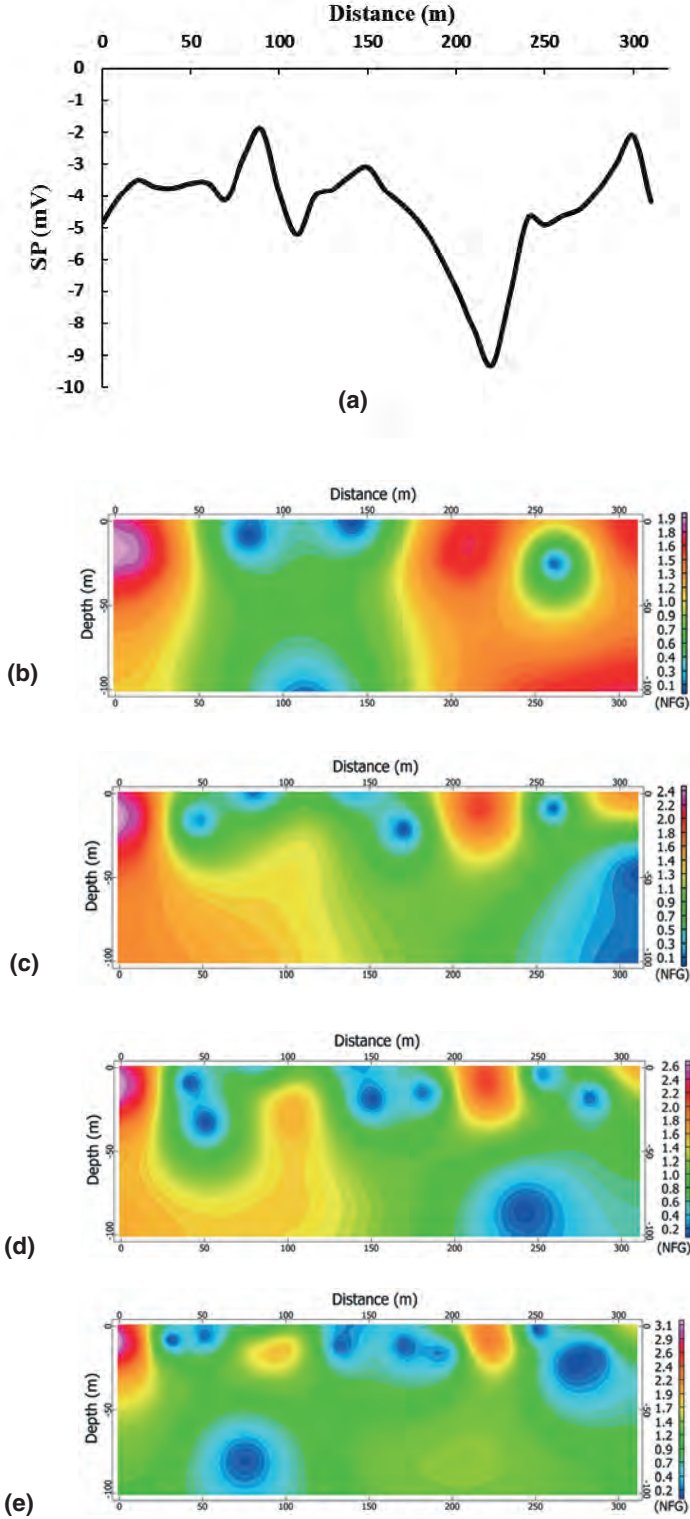


Fig. 11 - SP data modeling for profile 3, a) SP anomaly along  $x$  axis, b) NFG map for  $n=10$ , c) NFG map for  $n=15$ , d) NFG map for  $n=20$ , e) NFG map for  $n=25$ .

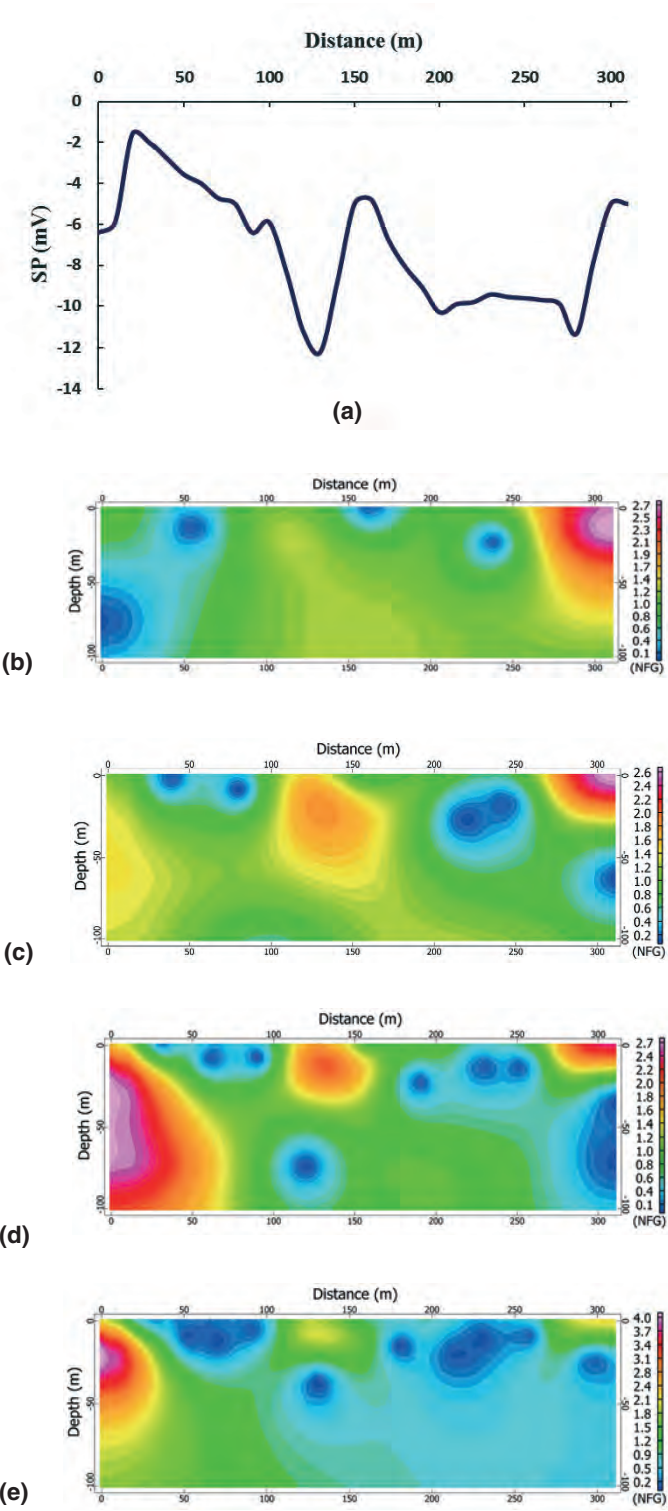


Fig. 12 - SP data for profile 4, a) SP anomaly along  $x$  axis, b) NFG map for  $n=10$ , c) NFG map for  $n=15$ , d) NFG map for  $n=20$ , e) NFG map for  $n=25$ .



(Esmaaili Oqaz, 1997). As is obvious from the SP anomaly map in Fig. 8, there are two sources of galena occurrence. Vein occurrence is exposed on the Earth surface in anomaly 1 but other source in anomaly 2 has deeper depth, and it should be better considered with other geophysical methods. Therefore, it is suggested using resistivity and induced polarization electrical profiles for detail study.

## 6. Conclusion

In this study, the application of a gradient based method to fast interpretation of potential data was considered for SP anomalies. In order to test the capability of this approach, sheet bodies were examined. Different random noises were added to their anomalies due to the reality of SP prospect survey. Satisfactory results for theoretical bodies indicated the acceptable performance of the NFG method. This method also could identify multi sources anomalies along a profile. Therefore, real data field was considered by the NFG. SP anomaly map of galena deposit located in Khalf village, Iran was chosen. The 2D interpretation of SP anomalies was carried out. The results showed the center location of underground sources, and also depth range was determined. These results had good matching with other studies.

**Acknowledgement.** Authors gratefully would like to thank the Institute of Geophysics and Department of Mining Engineering, University of Tehran, for all their supports.

## REFERENCES

- Abdelrahman E.M. and Sharafeldin S.M.; 1997: *A least-squares approach to depth determination from self-potential anomalies caused by horizontal cylinders and spheres*. Geophys., **62**, 44-48.
- Abdelrahman E.M., Ammar A.A., Hassanein H.I. and Hafez M.A.; 1998: *Derivative analysis of SP anomalies*. Geophys., **63**, 890-897.
- Abdelrahman E.M., El-Araby H.M., Ammar A.A. and Hassanein H.I.; 1997: *A least-squares approach to shape determination from residual self-potential anomalies*. Pure Appl. Geophys., **150**, 121-128.
- Abdelrahman E.M., El-Araby H.M., Hassanein A.R. and Hafez M.A.; 2003: *New methods for shape and depth determinations from SP data*. Geophys., **68**, 1202-1210.
- Akgün M., Akçi Z., Pinar R. and Ankaya O.; 1996: *Quantitative interpretation of self-potential data using of power spectra*. Jeofizik, **10**, 21-28.
- Ardestani V.E.; 2004: *Detection of near-surface anomalies through 2-D normalized full gradient of gravity data*. J. Earth Space Phys., **30**, 1-6.
- Asfahani J. and Tlas M.; 2002: *A nonlinear programming technique for the interpretation of self-potential anomalies*. Pure Appl. Geophys., **159**, 1333-1343.
- Asfahani J. and Tlas M.; 2005: *A constrained nonlinear inversion approach to quantitative interpretation of self-potential anomalies caused by cylinders, spheres and sheet-like structures*. Pure Appl. Geophys., **162**, 609-624.
- Atchuta R.D., Babu R. and Silvakumar S.G.D.J.; 1982: *A Fourier transform method for the interpretation of self-potential anomalies due to two to two-dimensional inclined sheets of finite depth extent*. Pure Appl. Geophys., **120**, 365-374.
- Aydin A.; 1997: *Evaluation of gravity data in terms of hydrocarbon by normalized full gradient variation and statistic methods, model studies and application in Hasankale-Horosan Basin (Erzurum)*. Ph.D. Thesis, Karadeniz Technical Univ., Natural and Applied Sciences Institute, Trabzon, Turkey.
- Aydin A.; 2010: *Application of the Normalized Full Gradient (NFG) method to resistivity data*. Turk. J. Earth Sci., **19**, 513-526.
- Babu H.V.R. and Rao D.; 1988: *Inversion of self-potential anomalies in mineral exploration*. Comput. Geosci., **14**, 377-387.

- Berezkin W.M.; 1967: *Application of the full vertical gravity gradient to determination to sources causing gravity anomalies*. Expl. Geophys., **18**, 69-76, (in Russian).
- Berezkin W.M.; 1973: *Application of gravity exploration to reconnaissance of oil and gas reservoir*. Nedra Publishing House, Russia, (in Russian).
- Berezkin W.M.; 1998: *Full gradient method in geophysical prospecting*. Nedra Publishing House, Russia, (in Russian).
- Blakely R.J.; 1995: *Potential theory in gravity and magnetic applications*. Cambridge University Press, Cambridge, UK, 441 pp.
- Bracewell R.; 1984: *The Fourier transform and its applications*. McGraw-Hill Book Co., New York, USA.
- Buselli G. and Kanglin L.; 2001: *Groundwater contamination monitoring with multichannel electrical and electromagnetic methods*. J. Appl. Geophys., **48**, 11-23.
- Dondurur D.; 2005: *Depth estimates for slingram electromagnetic anomalies from dipping sheet-like bodies by the normalized full gradient method*. Pure Appl. Geophys., **161**, 2179-2196.
- El-Araby H.M.; 2004: *A new method for complete quantitative interpretation of self-potential anomalies*. J. Appl. Geophys., **55**, 211-224.
- El-Kaliouby H.M. and Al-Garni M.A.; 2009: *Inversion of self-potential anomalies caused by 2D inclined sheets using neural networks*. J. Geophys. Eng., **6**, 29-34.
- Esmaaili Oqaz H.; 1997: *Quantitative and qualitative interpretation of self-potential anomalies due to polarized inclined sheet*. M.Sc. Thesis, Institute of Geophysics, University of Tehran, Iran, (published in Persian).
- Friedel S., Byrdina S., Jacobs F. and Zimmer M.; 2004: *Self-potential and ground temperature at Merapi volcano prior to its crisis in the rainy season of 2000-2001*. J. Volcanol. Geotherm. Res., **134**, 149-168.
- Karsli H.; 2001: *The usage of normalized full gradient method in seismic data analysis and a comparison to complex envelope curves*. Ph.D. Thesis, Karadeniz Technical University, Trabzon, Turkey (unpublished).
- Rao D. and Babu H.V.R.; 1983: *Quantitative interpretation of self-potential anomalies due to two- dimensional sheet – like bodies*. Geophys., **48**, 1659-1664.
- Rikitake T., Sato R. and Hagiwara Y.; 1976: *Applied mathematics for earth scientists*. Terra Scientific Publishing Co., Tokyo, Japan.
- Shalivahan, Bhattacharya B.B. and Mrinal K.S.; 1998: *Interpretation of self-potential anomalies by nonlinear inversion*. Geophys., **19**, 219-224.
- Sindirgi P., Pamukc U.O. and Özyalin S.; 2008: *Application of normalized full gradient method to Self Potential (SP) data*. Pure Appl. Geophys., **165**, 409-427.
- Sundararajan N. and Srinivas Y.; 1996: *A modified Hilbert transform and its application to self-potential interpretation*. J. Appl. Geophys., **36**, 137-143.
- Sundararajan N., Kumar A.I., Mohan N.L. and Seshagiri R.S.V.; 1990: *Use of Hilbert transform to interpret self-potential anomalies due to two-dimensional inclined sheets*. Pure Appl. Geophys., **133**, 117-126.
- Sundararajan N., Srinivasa R.P. and Sunitha V.; 1998: *An analytical method to interpret self-potential anomalies caused by 2-D inclined sheets*. Geophys., **63**, 1551-1555.
- Tlas M. and Asfahani J.; 2007: *A best-estimate approach for determining self-potential parameters related to simple geometric shaped structures*. Pure Appl. Geophys., **164**, 2313-2328.
- Xiao Y.; 1981: *Normalized Full Gradient Method of gravity anomalies*. Oil Geophys. Prospect., **16**, 47-57. (in Chinese).
- Xiao Y. and Zhang L.; 1984: *Application of normalized Full Gradient Method of gravity anomalies to oil and gas exploration*. Oil Geophys. Prospect., **19**, 247- 254. (in Chinese).
- Yungul S.; 1950: *Interpretation of spontaneous polarization anomalies caused by spherical ore bodies*. Geophys., **15**, 237-246.
- Zeng H., Meng X., Yao CH., Li X., Lou H., Guang Z. and Li Z.; 2002: *Detection of reservoirs from normalized Full Gradient of gravity anomalies and its application to Shengli Oil Field, East China*. Geophys., **67**, 1138-1147.

Corresponding author: Maysam Abedi  
Faculty of Mining Engineering, University of Tehran, Iran  
Phone: +98 09173124132; e-mail: maysamabedi@ut.ac.i